that the distribution of PAHs were determined for six sizes of airborne particles in Spain (Gutiérrez-Dabán *et al*, 2005). Their paper showed PAHs accumulated at higher percentages in the finest size range of submicron particles (smaller than 0.6 μm). It suggested that the existence of PAHs might relate to the number of benzene rings. For example, pyrene composed of four benzene rings, it easily adsorbed on the particle. Biphenyl, composed two benzene rings, exists as a gas. This present study did not use a quartz filter; the samples were collected through a membrane (<0.45 μm), and were adsorbed on Porapak-QS because the collected samples might contain particles <0.45 μm and gaseous substances. In this study pyrene was found in significantly higher levels in high traffic areas. Four PAHs (< 0.45 μm) were adsorbed and the other one may be a GOC. Some compounds were found on GC/MS analysis.

The detected compounds of GOC were DEB and DEB derivatives (Table 1). It has been reported that 1,2-DAB was metabolite of 1,2-DEB which behaves as a neurotoxin and a blue chromogen was induced (Gagnaire *et al*, 1990, 1991; Kim *et al*, 2002; Spencer *et al*, 2002; Tshala-Katumbay *et al*, 2005). 1,2-DEB is a moderately volatile, colorless liquid found in gasoline, kerosene, and fuel oil. A metabolic pathway of 1,2-DEB has been proposed that metabolizes to 1,2-EPE by ω-1 oxydation and forms 1,2-EPE and 1,2-DAB in rats (Payan *et al*, 1999).

ACKNOWLEDGEMENT

This work was supported by a Grant-in-Aid for Researchers, Hyogo College of Medicine, 2005.

REFERENCES

De Leon SF, Thurston GD, Ito K. Contribution of respiratory disease to nonrespiratory mortality associations with air pollution. *Am J Respir Crit Care Med* 2003; 167: 1117-23.

Dockery DW, Pope III CA, Xu X, *et al*. An association between air pollution and mortality in six U.S. cities. *N Engl J Med* 1993; 329: 1753-9.

Gagnaire F, Marignac B, de Ceaurriz J. Diethylbenzene-induced sensorimotor neuropathy in rats. *J Appl Toxicol* 1990; 10: 105-12.

Gagnaire F, Ensminger A, Marignac B, De Ceaurriz J. Possible involvement of 1, 2-diacetylbenzene in diethylbenzene-induced neuropathy in rats. *J Appl Toxicol* 1991; 11: 261-8.

Gutiérrez-Dabán A, Fernádez-Espinosa AJ, Ternero-Rodriguez M, Fernádez-Álvarez F. Particle size distribution of polycyclic aromatic hydrocarbons in urban air in southern Spain. *Anal Bioanal Chem* 2005; 381: 721-36.

Iavicoli I, Charotti M, Bergamaschi A, Marsili R, Carelli G. Determination of airborne polycyclic aromatic hydrocarbons at an airport by gas chromatography-mass spectrometry and evaluation of occupational exposure. *J Chromatogr* 2006; 1150: 226-35.

Kim MS, Hashemi SB, Spencer PS, Sabri MI. Amino acid and protein targets of 1,2-diethylbenzene, a potent aromatic γ-diketone that induces proximal neurofilamentous axonopathy. *Toxicol Appl Pharmacol* 2002; 183: 55-65.

Laden F, Neas LM, Dockery DW, Schwatz J. Association of fine particulate matter from different sources with daily mortality in six US cities. *Environ Health Perspect* 2000; 108: 941-7.

Payan J-P, Beydon D, Cossec B, Ensminger A, Fabry J-P, Ferrari E. Toxicokinetics of 1,2-diethylbenzene in male sprague-dawley rats - Part 1: Excretion and metabolism of [14C]1,2-diethylbenzene. *Drug Metab Disposit* 1999; 27: 1470-78.

Pellizzari, ED, Bunch, JE, Carpenter, BH, Sawicki, EBH. Collection and analysis of trace organic vapor pollutants in ambient atmosphere. *Environ Sci Technol* 1975; 9: 552-5.

Penning TM, Burczynski ME, Hung CF, McCoull KD, Palackal NT, Tsuruda LS. Dihydrodiol dehydrogenases and polycyclic aromatic hydrocarbon activation: generation of reactive and redox

active o-quinones. *Chem Res Toxicol* 1999; 12: 1-18.

Pope III CA, Burnett RT, Thurston GD, *et al*. Cardiovascular mortality and long-term exposure to particulate air pollution. *Circulation* 2004; 109: 71-7.

Samet JM, Dominici F, Curriero FC, Coursac I, Zeger SL. Fine particulate air pollution and mortality in 20 U.S. cities, 1987-1994. *N Engl J Med* 2000; 343: 1742-9.

Spencer PS, Kim MS, Sabri MI. Aromatic as well as aliphatic hydrocarbon solvent axonopathy. *Int J Hyg Environ Health* 2002; 205: 131-6.

Tshala-Katumbay DD, Palmer VS, Kayton RJ. A new murine model of giant proximal axonopathy. *Acta Neuropathol* 2005; 109: 405-10.

Xia T, Korge P, Weiss JN, Li N, Venkatesen MI, Sioutas C. Quinones and aromatic chemical compounds in particulate matter induce mitochondrial dysfunction: implications for ultrafine particle toxicity. *Environ Health Perspect* 2004; 112: 1347-58.

PULMONARY EXPOSURE TO CARBON BLACK NANOPARTICLES INCREASES THE NUMBER OF ANTIGEN-PRESENTING CELLS IN MURINE LUNG

E. KOIKE, H. TAKANO, K.-I. INOUE, R. YANAGISAWA, M. SAKURAI, H. AOYAGI[1], R. SHINOHARA[2] and T. KOBAYASHI

Environmental Health Sciences Division, National Institute for Environmental Studies, Onogawa, Tsukuba, Ibaraki; [1]Biosystem Studies and [2]Life and Environmental Sciences, University of Tsukuba, Tsukuba, Ibaraki, Japan

Received April 12, 2007 – Accepted September 7, 2007

Particulate matters can enhance antigen-related airway inflammation and immunoglobulin production. The present study was designed to determine the effects of different sizes of nanoparticles on the antigen-presenting cells (APC) in the lung. ICR mice were exposed to vehicle, carbon black (CB) nanoparticles (14 nm or 56 nm), ovalbumin (OVA), or OVA+nanoparticles intratracheally. The expression of major histocompatibility complex (MHC) class II, costimulatory molecules (CD80, CD86, CD11c), and DEC205 (dendritic cell marker), F4/80 (macrophage marker), and CD19 (B-cell marker) in the lung cells was measured by flow cytometry. 14 nm nanoparticles, but not 56 nm nanoparticles, increased the number of the total lung cells. Combination of OVA and 14 nm or 56 nm nanoparticles increased the total lung cells. The expression of MHC class II and/or costimulatory molecules and the number of APC in the lung were increased by 14 nm nanoparticles in the presence or absence of OVA. The increases were more prominent with combination of OVA and 14 nm nanoparticles. 56 nm nanoparticles did not show any significant effects. 14 nm CB nanoparticles can increase the expression of MHC class II and costimulatory molecules and the number of APC in the lung, especially in the presence of antigen, which can result in subsequent antigen-related airway inflammation and immunoglobulin production.

Epidemiological studies have shown an association between increased particulate air pollution and adverse health effects on susceptible individuals, including the elderly with respiratory and cardiovascular diseases (1-3). Particulate matters with an aerodynamic diameter of 2.5 μm or less (PM2.5) are more closely associated with acute and chronic respiratory effects and subsequent mortality than PM with an aerodynamic diameter of 10 μm or less (PM10) (4).

Ultrafine particles (UFPs) with a diameter of <0.1 μm represent a substantial component, in terms of particle numbers, in PM10 and/or PM2.5, although they represent a relatively small fraction of the total mass. The respiratory effects of the number of the UFPs are stronger than those of PM10 (4). In long-term, high-dose exposure, UFPs have been shown to cause chronic pulmonary inflammation, increased chemokine expression, epithelial cell hyperplasia, pulmonary fibrosis, and lung tumor (5-7). UFPs are able to penetrate deeply into the respiratory tract, and they have a larger surface area than larger particles, thus causing a greater inflammatory response (8-9).

Key words: antigen-presenting cells, antigen-related airway inflammation, carbon black nanoparticles, costimulatory molecules, major histocompatibility complex class II molecules

Mailing address: Hirohisa Takano, MD, PhD
Environmental Health Sciences Division,
National Institute for Environmental Studies,
16-2 Onogawa, Tsukuba,
305-8506, Japan
Tel/Fax: ++81 29 850 2334
e-mail: htakano@nies.go.jp

0394-6320 (2008)

Our previous study demonstrated that carbon black (CB) nanoparticles with a diameter of 14 nm or 56 nm can aggravate antigen-related airway inflammation by infiltration of inflammatory cells and an increase in the number of goblet cells, and immunoglobulin production. The CB nanoparticles also induce the inflammatory cytokine and chemokine protein levels in the lung tissue, and the expression of 8-hydroxy-2'-deoxyguanosine, an oxidative marker in the lung cells phagocyting nano particles. These CB nanoparticle-mediated aggravations are more prominent with smaller particles (10). In particular, the levels of antigen-specific IgG_1 and IgE are significantly greater in the antigen+14 nm nanoparticle group.

Enhancement of antigen-presenting activity can lead to the increase of antigen-related immunoglobulin production and allergic airway inflammation through the proliferation and activation of lymphocytes and eosinophils. Therefore, the expression of cell surface molecules associated with antigen presentation and/or the number of antigen-presenting cells (APC) should be important in the possible mechanisms of the aggravation of allergic responses. Major histocompatibility complex (MHC) class II molecules (11) and co-stimulatory molecules such as CD80, CD86, CD11b or CD11c (12-14) are necessary for antigen presentation. MHC class II is expressed on the dendritic cells (DC), macrophages, or B-cells: those playing a role of APC in the lung tissue.

We hypothesized that nanoparticles recruit and activate APC in the lung, as a possible mechanism in the aggravation of allergic responses and inflammation. Our present study was designed to determine the effects of two sizes of CB nanoparticles (14 nm and 56 nm) on the expression of MHC class II and co-stimulatory molecules and the number of DC, macrophages, and B cells in the lung.

MATERIALS AND METHODS

Animals

Specific pathogen-free, male ICR mice (5 wk of age) were obtained from CLEA Japan Inc. (Tokyo, Japan) and were used at 6 wk of age (weighing 29 to 33 g). The animals were given sterile distilled water and CE-2 food (CLEA Japan Inc.) *ad libitum*. Mice were housed in an animal facility that was maintained at 24-26°C with 55-75% humidity and a 12 h light/dark cycle.

Nanoparticles

CB nanoparticles with a diameter of 14 nm (Printex 90) and 56 nm (Printex 25) were obtained from Degussa (Dusseldorf, Germany). The surface area of the 14 nm nanoparticles was 300 m^2/g and that of the 56 nm nanoparticles was 45 m^2/g. Nanoparticles were autoclaved at 250°C for 2 h in an electric heater before use. The nanoparticle suspension was sonicated for 3 min using an ultrasonic disrupter (UD-201; Tomy Seiko, Tokyo, Japan).

Study protocol

Mice were divided into six experimental groups (n=4 in each group). The vehicle group received Dulbecco's calcium and magnesium-free, phosphate-buffered saline (PBS) at pH 7.4 (Nissui Pharmaceutical Co., Tokyo, Japan) containing 0.05% Tween 80 (Nakalai Tesque, Kyoto, Japan) once a week for 6 wk. The ovalbumin (OVA) group received 1 μg of OVA (Sigma Chemical, St. Louis, MO) dissolved in the same vehicle every 2 wk for 6 wk. The nanoparticle groups received 50 μg of 14 nm or 56 nm CB nanoparticles suspended in the same vehicle every week for 6 wk. The OVA+nanoparticle groups received the combined treatment in the same protocol as the OVA and the nanoparticle groups, respectively. In each group, vehicle, OVA, nanoparticles, or OVA+nanoparticles was dissolved in 0.1 ml aliquots, and inoculated by the intratracheal route through a polyethylene tube under anesthesia with 4% halothane (Hoechst, Japan, Tokyo, Japan). The animals were studied 4 h after the last intratracheal administration, with the expression of cell surface molecules associated with antigen presentation in the lung cells.

Preparation of the lung cells

Mice were anesthetized with sodium pentobarbital (Dainippon Pharmaceutical Co., Osaka, Japan) given intraperitoneally (50 mg/kg), and exsanguinated from the cut abdominal aorta and vein. The lung cells were prepared as previously described (15). Briefly, the lung vessel was perfused with 2 ml of chilled PBS containing 0.2% bovine serum albumin (BSA) and 10 U/ml heparin introduced into the right ventricle. The lung tissue was sliced and was digested for 90 min at 37°C in 2 ml of PBS containing 0.2% BSA, 0.25 mg/ml collagenase A, and 50 U/ml DNAase I. After teasing the digested tissue and after filtration through cotton wool, single cell suspensions were collected. The numbers of viable cells were determined by the trypan blue (Gibco Laboratories, Grand Island, NY) exclusion method.

FACS analysis

For FACS analysis, the following monoclonal antibodies were used: MHC class II molecules: I-A/I-E (2G9, FITC-

conjugated, BD Biosciences Pharmingen, CA); costimulatory molecules: CD80 (16-10A1, PE-conjugated, BD Biosciences Pharmingen), CD86 (GL1, PE-conjugated, BD Biosciences Pharmingen), CD11c (HL3, PE-conjugated, BD Biosciences Pharmingen); DC marker: DEC-205 (NLDC-145, PE-conjugated, Cedarlane Labs, Ontario, Canada); macrophage marker: F4/80 (CI:A3-1, PE-conjugated, Serotec, Oxford, UK); B-cell differentiation antigen: CD19 (6D5, PE-conjugated, Southern Biotechnology, Birmingham, AL). Cells (1×10^6) were resuspended in 100 µl PBS with 0.3% BSA and 0.05% sodium azide (Wako Pure Chemical Industries, Osaka, Japan) and were stained with antibodies at 1 µg for 30 min on ice. After incubation, the cells were washed, and the fluorescence was measured by a FACSCalibur (Becton, Dickinson and Company, NJ). Fluorescence data were expressed as the percentage of positive cells. The numbers of cells expressing each cell surface molecule in murine lung were represented.

Statistical analysis

Data were represented as the mean ± SEM of four animals. Differences between groups were determined using ANOVA with post hoc test (StatView J-4.5; Abacus Concepts, Inc., Berkeley, CA). A p value of <0.05 was considered to indicate a significant difference between pairs of groups.

RESULTS

The number of total lung cells

The numbers of total cells in the lung were significantly greater in the 14 nm nanoparticle and the OVA+14 nm nanoparticle groups than in the vehicle group (Table I: $p<0.05$). The number of total lung cells was also greater in the OVA+56 nm nanoparticle group than in the vehicle group, but the difference did not achieve significance. Challenge with 56 nm nanoparticles or OVA alone did not increase the total lung cells as compared to vehicle challenge. The numbers of total lung cells were significantly greater in the OVA+nanoparticle groups than in the OVA group ($p<0.01$ for OVA+14 nm nanoparticles, $p<0.05$ for OVA+56 nm nanoparticles). Challenge with nanoparticles, OVA, and OVA+nanoparticles did not affect the viability of the lung cells.

The expression of MHC class II and costimulatory molecules

The number of MHC class II^+ cells was significantly greater in the 14 nm nanoparticle and the OVA+14 nm nanoparticle groups than in the vehicle group (Fig. 1A: $p<0.01$). The number of the cells was even greater in the OVA+14 nm nanoparticle group than in the 14 nm nanoparticle or the OVA group ($p<0.01$). The percentages of the expression of MHC class II in total lung cells from the vehicle, 14 nm nanoparticle, 56 nm nanoparticle, OVA, OVA+14 nm nanoparticle, and OVA+56 nm nanoparticle groups were 3.5±0.7, 8.6±3.1, 3.4±0.73, 3.1±1.1, 10.9±1.4, and 2.4±1.1%, respectively. Challenge with 56 nm nanoparticles, OVA, or OVA+56 nm nanoparticles did not increase the expression and the number of MHC class II^+ cells in the lung as compared to vehicle challenge (Fig. 1A).

The numbers of $CD80^+$ and $CD86^+$ cells were significantly greater in the 14 nm nanoparticle ($p<0.05$ for $CD80^+$ cells, $p<0.01$ for $CD86^+$ cells) and the OVA+14 nm nanoparticle ($p<0.01$) groups than in the vehicle group (Fig. 1B and 1C). The numbers of the cells were further increased in the OVA+14 nm nanoparticle group than in the 14 nm nanoparticle or the OVA group ($p<0.01$). Furthermore, the numbers of MHC class II^+ $CD80^+$ and MHC class II^+ $CD86^+$ cells were also increased by challenge with 14 nm nanoparticles ($p<0.01$ versus vehicle) or OVA+14 nm nanoparticles ($p<0.01$ versus vehicle, OVA, or 14 nm nanoparticles) in the same manner as those of $CD80^+$ and $CD86^+$ cells (Fig. 1B and 1C). The numbers of $CD11c^+$ and MHC class II^+ $CD11c^+$ cells were significantly greater in the 14 nm nanoparticle and the OVA+14 nm nanoparticle groups than in the vehicle group (Fig. 1D: $p<0.05$). However, challenge with OVA+14 nm nanoparticles did not further increase the cell numbers as compared with 14 nm nanoparticles or OVA alone.

The number of DC, macrophages, and B cells

The number of cells expressing DEC205 as a marker of DC was significantly greater in the OVA+14 nm nanoparticle group than in the vehicle or the OVA group (Fig. 2A: $p<0.05$). The cells were also increased by 14 nm nanoparticles alone, but which did not show significance versus vehicle. The number of MHC class II^+ $DEC205^+$ cells was increased by challenge with OVA+14 nm nanoparticles in the same manner as that of $DEC205^+$ cells (Fig. 2A: $p<0.05$ versus vehicle or OVA). Furthermore, most $DEC205^+$ cells expressed MHC class II molecules. The number of cells expressing

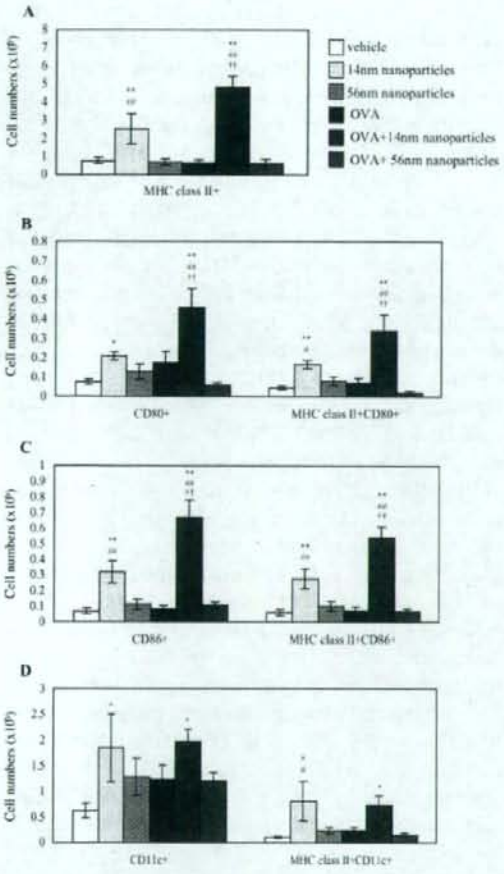

Fig. 1. *Effects of nanoparticles on the number of cells expressing MHC class II and costimulatory molecules in the lung. Six groups of mice were intratracheally administered with vehicle, ovalbumin (OVA), carbon black nanoparticles, or OVA+nanoparticles for 6 wk. Lung cells were prepared 4 h after the last intratracheal instillation. The expression of cell surface molecules was analyzed by flow cytometry. The number of each cell type in the lung was shown: (A) MHC class II, (B) MHC class II and CD80, (C) MHC class II and CD86, (D) MHC class II and CD11c. Values are presented as mean ± SEM of 4 animals. *P<0.05, **P<0.01 versus vehicle; †P<0.05, ††P<0.01 versus OVA; ‡P<0.05, ‡‡P<0.01 versus nanoparticles.*

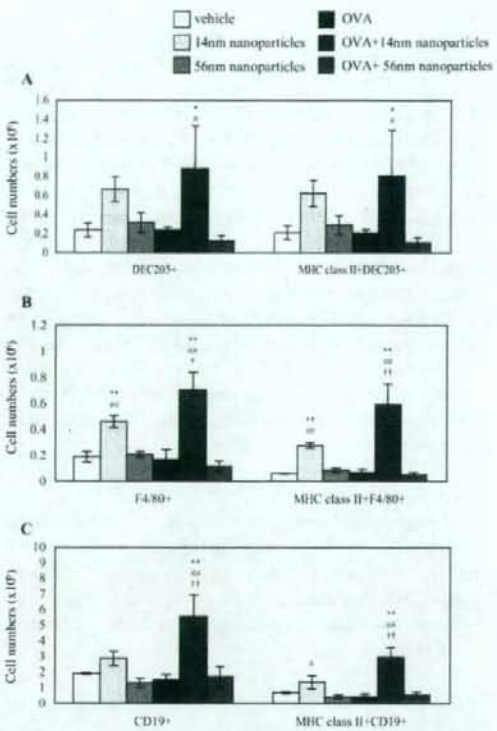

Fig. 2. *Effects of nanoparticles on the number of APC in the lung tissue. Six groups of mice were intratracheally administered with vehicle, OVA, nanoparticles, or OVA+nanoparticles for 6 wk. Lung cells were prepared 4 h after the last intratracheal instillation. The expression of cell surface molecules was analyzed by flow cytometry. The number of each cell type in the lung was shown: (A) MHC class II and DEC205 as a maker of dendritic cells, (B) MHC class II and F4/80 as a maker of macrophages, (C) MHC class II and CD19 as a maker of B cells. Values are presented as mean± SEM of 4 animals. *P<0.05, **P<0.01 versus vehicle; †P<0.05, ††P<0.01 versus OVA; ‡P<0.05, ‡‡P<0.01 versus nanoparticles.*

F4/80 as a maker of macrophages was significantly greater in the 14 nm nanoparticle and the OVA+14 nm nanoparticle groups than in the vehicle group (Fig. 2B: $p<0.01$). The number of the cells was further increased in the OVA+14 nm nanoparticle group than in the 14 nm nanoparticle ($p<0,05$) or the OVA ($p<0.01$) group. The number of MHC class II^+ $F4/80^+$ cells was also increased by challenge

Table I. *Effects of nanoparticles on the number of total cells in the lung. Six groups of mice were intratracheally administered with vehicle, ovalbumin (OVA), carbon black nanoparticles, or combinations of OVA and nanoparticles for 6 wk. Lung was removed 4 h after the last intratracheal instillation. The lung tissue was digested and lung cells were collected. Total cell counts and cell viability were determined by the trypan blue exclusion method.*

Group	Body weight (g)	Number of total cells ($1x10^7$/lung tissue)	Cell viability (%)
vehicle	36.18±0.85	2.225±0.103	96.45±0.82
14nm nanoparticles	39.07±2.35	3.298±0.518$^{*\#}$	96.19±1.08
56nm nanoparticles	37.34±1.19	2.043±0.263	96.56±0.50
OVA	39.11±1.42	2.092±0.293	96.85±0.79
OVA+14nm nanoparticles	39.29±1.50	3.278±0.556$^{*\#\#}$	97.44±0.78
OVA+56nm nanoparticles	40.20±2.07	3.123±0.438$^{\#}$	97.00±1.11

Results are presented as mean ± SEM. $^{*}P < 0.05$ versus vehicle, $^{\#}P < 0.05$, $^{\#\#}P < 0.01$ versus OVA

with 14 nm nanoparticles ($p<0.01$ versus vehicle) or OVA+14 nm nanoparticles ($p<0.01$ versus vehicle, OVA, or 14 nm nanoparticles) in the same manner as that of F4/80$^+$ cells (Fig. 2B). The number of cells expressing CD19 as a marker of B-cells was significantly greater in the OVA+14 nm nanoparticle group than in the vehicle, the 14 nm nanoparticle, or the OVA group (Fig. 2C: $p<0.01$). The cells were also increased by 14 nm nanoparticles alone, but did not achieve significance versus vehicle. The number of MHC class II$^+$ CD19$^+$ cells was increased by challenge with OVA+14 nm nanoparticles in the same manner as that of CD19$^+$ cells (Fig. 2C: $p<0.01$ versus vehicle, OVA, or 14 nm nanoparticles).

DISCUSSION

We previously reported that CB nanoparticles aggravate antigen-related airway inflammation and immunoglobulin production, which is more prominent with smaller particles (10). To elucidate the mechanisms of the aggravation, the current study investigates the effects of the nanoparticles on APC in the lung. The present results demonstrate that 14 nm CB nanoparticles administered by the intratracheal route enhance the expression of MHC class II and costimulatory molecules and the number of APC in the presence or absence of antigen in murine lung. Strikingly, the enhancement is more prominent in the presence of antigen.

Previous *in vitro* studies have reported that human monocytes up-regulate the expression of HLA-DR and costimulatory molecules in response to PM (16) and rat monocytes up-regulate the expression of Ia and costimulatory molecules and antigen-presenting activity in response to DEP (17). In addition, our previous *in vivo* studies have demonstrated that O_3 exposure increases Ia and costimulatory molecules and antigen-presenting activity in rat bronchoalveolar lavage cells (18) and lung interstitial cells (15). However, it has not been elucidated whether nanoparticles affect the lung APC, especially *in vivo*. The present results should be the first *in vivo* demonstration that CB nanoparticles can enhance the expression of MHC class II and costimulatory molecules and the number of APC in the lung.

We used CB as an elemental carbon in the present study, since CB is relatively inert, and the effects of particle size can be elucidated without confounding

factors (19). Exposure to the ultrafine but not fine CB alone has caused an increase in airway inflammation (20). Previously, we focused on the effects of particle size on antigen-related airway inflammation, and demonstrated that CB nanoparticles can aggravate antigen-related airway inflammation characterized by infiltration of inflammatory leukocytes, and increase the expression of interleukin (IL)-5, IL-13, eotaxin, monocyte chemoattractant protein (MCP)-1, and regulated on activation and normal T cells expressed and secreted (RANTES) in the lung (10). The enhancing effects are more prominent with 14 nm nanoparticles than with 56 nm nanoparticles. Furthermore, the administration of 14 nm nanoparticles with antigen has significantly enhanced the production of antigen-specific IgG1 and IgE. These results clearly indicate that smaller particles have greater effects on antigen-related airway inflammation.

Enhancement of antigen-presenting activity can lead to the increase of immunoglobulin production and allergic airway inflammation through the proliferation and activation of lymphocytes and eosinophils. In the present study, the numbers of cells expressing MHC class II and/or costimulatory molecules (CD80, CD86, CD11c) in the lung were increased by the administration of 14 nm nanoparticles or OVA+14 nm nanoparticles (Fig. 1). The interaction of APC, T-cells, and B-cells is necessary for antigen-specific responses including immunoglobulin production and recruitment of inflammatory cells. The increase in activated B-cells may lead to maturation of IgE-positive B-cells to IgE-producing plasma cells. In the present study, the numbers of DC, macrophages, and B-cells in the lung were also increased by the administration of 14 nm nanoparticles or OVA+14 nm nanoparticles (Fig. 2). The increases were more prominent in the OVA+14 nm nanoparticle group than in the 14nm nanoparticle or the OVA group. Previous reports and the present results indicate that the recruitment and activation of APC by nanoparticles can, at least partially, mediate the aggravation of airway responses and inflammation related to antigen. In fact, in the present study, the effects of nanoparticles were markedly greater in the presence of antigen.

It has been demonstrated that DC isolated from parenchymal lung tissue exhibits strong antigen-presenting activity *in vitro* (21-23), although they represent a relatively small number of the lung tissue. In the present study, the number of DC was larger than that of macrophages. Furthermore, most DC expressed MHC class II molecules (Fig. 2A), therefore, DC should be the important APC at least in this system.

In our previous study (10), nanoparticles significantly increased the level of MCP-1 and RANTES in the lung. Furthermore, a recent study demonstrates that nanoparticles also elevate the level of macrophage inflammatory protein (MIP)-1α, granulocyte-macrophage colony-stimulating factor (GM-CSF) and IL-2 in the lung (24). RANTES, MIP-1α and IL-2 play a role in the recruitment of DC into the lung, and GM-CSF promotes the activation of DC. Therefore, the enhancement of the expression of MHC class II and costimulatory molecules mediated by nanoparticles might be caused by the increase of these cytokine and chemokine levels.

It has been demonstrated that oxidative stress induces phenotypic and functional maturation of DC as an APC (25-26). Our previous study showed that the expression of 8-hydroxy-2'-deoxyguanosine, as a proper marker of the oxidative stress, in the lung was more intense in the OVA+nanoparticle groups than in the OVA group (10). Also, in our recent study, we assessed the innate oxidative capacity of CB nanoparticles in a cell-free system. The nanoparticles had oxidative capacity and the capacity of 14 nm nanoparticles was greater than that of 56 nm (27). It is suggested that the oxidative stress would be a key component causing the effects of nanoparticles on the enhanced APC activation. In conclusion, exposure to 14 nm CB nanoparticles can enhance the expression of MHC class II and/or costimulatory molecules and the number of APC in the lung, which can contribute to the enhancement of antigen-related immunoglobulin production and airway inflammation.

REFERENCES

1. **Gilmour P.S., D.M. Brown, T.G. Lindsay, P.H. Beswick, W. MacNee and K. Donaldson.** 1996. Adverse health effects of PM10 particles: involvement of iron in generation of hydroxyl radical. *Occup. Environ. Med. 53:817.*

2. **Donaldson K., V. Stone, A. Seaton and W. MacNee.** 2001. Ambient particle inhalation and the cardiovascular system: potential mechanisms. *Environ. Health Perspect. 109:523.*
3. **MacNee W. and K. Donaldson.** 2003. Mechanism of lung injury caused by PM10 and ultrafine particles with special reference to COPD. *Eur. Respir. J. 40(S): 47.*
4. **Peters A., H.E. Wichmann, T. Tuch, J. Heinrich and J. Heyder.** 1997. Respiratory effects are associated with the number of ultrafine particles. *Am. J. Respir. Crit. Care Med. 155:1376.*
5. **Oberdorster G., J. Ferin and B.E. Lehnert.** 1994. Correlation between particle size, *in vivo* particle persistence, and lung injury. *Environ. Health Perspect. 102:173.*
6. **Dasenbrock C., L. Peters, O. Creutzenberg and U. Heinrich.** 1996. The carcinogenic potency of carbon particles with and without PAH after repeated intratracheal administration in the rat. *Toxicol. Lett. 88:15.*
7. **Driscoll K.E., J.M. Carter, B.W. Howard, D.G. Hassenbein, W. Pepelko, R.B. Baggs and G. Oberdorster.** 1996. Pulmonary inflammatory, chemokine, and mutagenic responses in rats after subchronic inhalation of carbon black. *Toxicol. Appl. Pharmacol. 136: 372.*
8. **Donaldson K., D. Brown, A. Clouter, R. Duffin, W. MacNee, L. Renwick, L. Tran and V. Stone.** 2002. The pulmonary toxicology of ultrafine particles. *J. Aerosol Med. 15:213.*
9. **Oberdorster G.** 2001. Pulmonary effects of inhaled ultrafine particles. *Int. Arch. Occup. Environ. Health 74:1.*
10. **Inoue K., H. Takano, R. Yanagisawa, M. Sakurai, T. Ichinose, K. Sadakane and T. Yoshikawa.** 2005. Effects of nanoparticles on antigen-related airway inflammation in mice. *Respir. Res. 6:106.*
11. **Niederhuber J.E. and D.C. Shreffler.** 1977. Anti-Ia serum blocking of macrophage function in the *in vitro* humoral response. *Transplant Proc. 9:875.*
12. **Lenschow D.J., G.H. Su, L.A. Zuckerman, N. Nabavi, C.L. Jellis, G.S. Gray, J. Miller and J.A. Bluestone.** 1993. Expression and functional significance of an additional ligand for CTLA-4. *Proc. Natl. Acad. Sci. USA 90:11054.*
13. **Freeman G.J., F. Borriello, R.J. Hodes, H. Reiser, J.G. Gribben, J.W. Ng, J. Kim, J.M. Goldberg, K. Hathcock, G. Laszlo, L.A. Lonbard, S. Wang, G.S. Gray, L.M. Nadler and A.H. Sharpo.** 1993. Murine B7-2, an alternative CTLA4 counter-receptor that costimulates T cell proliferation and interleukin 2 production. *J. Exp. Med. 178:2185.*
14. **Meunier L., K. Bohjanen, J.J. Voorhees and K.D. Cooper.** 1994. Retinoic acid upregulates human Langerhans cell antigen presentation and surface expression of HLA-DR and CD11c, a beta 2 integrin critically involved in T-cell activation. *J. Invest. Dermatol. 103:775.*
15. **Koike E. and T. Kobayashi.** 2004. Ozone exposure enhances antigen-presenting activity of interstitial lung cells in rats. *Toxicology 196:217.*
16. **Becker S. and J. Soukup.** 2003. Coarse(PM(2.5-10)), fine(PM(2.5)), and ultrafine air pollution particles induce/increase immune costimulatory receptors on human blood-derived monocytes but not on alveolar macrophages. *J. Toxicol. Environ. Health 66:847.*
17. **Koike E. and T. Kobayashi.** 2005. Organic extract of diesel exhaust particles stimulates expression of Ia and costimulatory molecules associated with antigen presentation in rat peripheral blood monocytes but not in alveolar macrophages. *Toxicol. Appl. Pharmacol. 209:277.*
18. **Koike E., T. Kobayashi and N. Shimojo.** 2001. Ozone exposure enhances expression of cell-surface molecules associated with antigen-presenting activity on bronchoalveolar lavage cells in rats. *Toxicol. Sci. 63:115.*
19. **Lambert A.L., J.B. Mangum, M.P. DeLorme and J.I. Everitt.** 2003. Ultrafine carbon black particles enhance respiratory syncytial virus-induced airway reactivity, pulmonary inflammation, and chemokine expression. *Toxicol. Sci. 72:339.*
20. **Gilmour P.S., A. Ziesenis, E.R. Morrison, M.A. Vickers, E.M. Drost, I. Ford, E. Karg, C. Mossa, A. Schroeppel, G.A. Ferron, J. Heyder, M. Greaves, W. MacNee and K. Donaldson.** 2004. Pulmonary and systemic effects of short-term inhalation exposure to ultrafine carbon black particles. *Toxicol. Appl. Pharmacol. 195:35.*
21. **Holt P.G., M.A. Schon-Hegrad and J. Oliver.**

1988. MHC class II antigen-bearing dendritic cells in pulmonary tissues of the rat. Regulation of antigen presentation activity by endogenous macrophage populations. *J. Exp. Med. 167:262.*

22. **Rochester C.L., E.M. Goodell, J.K. Stoltenborg and W.E. Bowers.** 1988. Dendritic cells from rat lung are potent accessory cells. *Am. Rev. Respir. Dis. 138:121.*
23. **Sertl K., T. Takemura, E. Tschachler, V.J. Ferrans, M.A. Kaliner and E.M. Shevach.** 1986. Dendritic cells with antigen-presenting capability reside in airway epithelium, lung parenchyma, and visceral pleura. *J. Exp. Med. 163:436.*
24. **Inoue K., H. Takano, R. Yanagisawa, T. Ichinose, M. Sakurai and T. Yoshikawa.** 2006. Effects of nano particles on cytokine expression in murine lung in the absence or presence of allergen. Arch. Toxicol. *80:614.*
25. **Rutault K., C. Alderman, B.M. Chain and D.R. Katz.** 1999. Reactive oxygen species activate human peripheral blood dendritic cells. *Free Radic. Biol. Med. 26:232.*
26. **Kantengwa S., L. Jornot, C. Devenoges and L.P. Nicod.** 2003. Superoxide anions induce the maturation of human dendritic cells. *Am. J. Respir. Crit. Care Med. 167:431.*
27. **Koike E. and T. Kobayashi.** 2006. Chemical and biological oxidative effects of carbon black nanoparticles. *Chemosphere 65:946.*

Effects of Pulmonary Exposure to Carbon Nanotubes on Lung and Systemic Inflammation with Coagulatory Disturbance Induced by Lipopolysaccharide in Mice

KEN-ICHIRO INOUE,*[,1] HIROHISA TAKANO,* EIKO KOIKE,* RIE YANAGISAWA,* MIHO SAKURAI,* SADATOMO TASAKA,† AKITOSHI ISHIZAKA,† AND AKINORI SHIMADA‡

Environmental Health Sciences Division, National Institute for Environmental Studies, Ibaraki XXX-XXXX, Japan; †Division of Pulmonary Medicine, Keio University School of Medicine, Tokyo XXX-XXXX, Japan; and ‡Department of Veterinary Pathology, Faculty of Agriculture, Tottori University, Tottori XXX-XXXX, Japan

?1

Despite intensive research as to the pathogenesis of lipopolysaccharide (LPS)-related inflammation with coagulatory disturbance, their exacerbating factors have not been explored. This study examined the effects of pulmonary exposure to two types of nano-sized materials (carbon nanotubes: CNT [single-wall: SWCNT, and multi-wall: MWCNT]) on lung inflammation and consequent systemic inflammation with coagulatory disturbance induced by pulmonary exposure to LPS in mice and their cellular mechanisms *in vitro*. ICR male mice were divided into 6 experimental groups that intratracheally received the vehicle, two types of CNT (4 mg/kg), LPS (33 μg/kg), or LPS plus either type of CNT. Twenty-four hours after treatment, both types of CNT alone induced lung inflammation with enhanced lung expression of proinflammatory cytokines, but did not synergistically exacerbate lung inflammation elicited by LPS. SWCNT significantly induced/enhanced pulmonary permeability and hyperfibrinogenemia and reduced activated protein C in the absence or presence of LPS, whereas MWCNT did moderately. Both CNT moderately, but not significantly, elevated circulatory levels of proinflammatory cytokines and chemokines. In the presence of LPS, CNT tended to elevate the levels of the mediators with an overall trend, which was more prominent with SWCNT than with MWCNT. *In vitro* study showed that both CNT amplified LPS-induced cytokine production from peripheral blood monocytes. These results suggest that CNT can facilitate systemic inflammation with coagulatory disturbance, at least in part, via the activation of mononuclear cells, which is accompanied by moderate enhancement of acute lung inflammation related to LPS. Exp Biol Med 233:000–000, 2008

Key words: carbon nanotubes; lipopolysaccharide; lung inflammation; systemic inflammation; coagulatory disturbance

Introduction

Endotoxin (lipopolysaccharide: LPS) induces systemic inflammatory response syndrome (SIRS), such as acute lung and systemic inflammation/injury and multiple organ dysfunction, frequently accompanied by consumptive hemostatic changes and often leading to coagulopathy including disseminated intravascular coagulation (DIC) (1). Although intensive research into the pathogenesis of SIRS with or without DIC and other coagulopathy has been conducted, their exacerbating factors have not yet been explored. Epidemiologically, environmental particulate matters of mass median aerodynamic diameter (a density-dependent unit of measure used to describe the diameter of the particle) < or 2.5 μm ($PM_{2.5}$), including diesel exhaust particles (DEP) and nanoparticles (< 100 nm) relate to the induction/enhancement of cardiopulmonary diseases, including lung inflammation, allergic asthma, pulmonary emphysema, and ischemic (coronary) heart diseases (2–9). On the other hand, LPS is a significant constituent of many air pollutant particles and has accordingly been implicated in PM effects (10). To support these reports, we have previously demonstrated that DEP, their components (especially residual particles after extraction of chemical

This study was supported by Grants-in-Aid for Scientific Research (B) 18390188 from the Japan Society for the Promotion of Science.

The authors state that they have no conflicts of interest.

[1] To whom correspondence should be addressed at Environmental Health Sciences Division, National Institute for Environmental Studies, 16–2 Onogawa, Tsukuba 305-8506, Japan. E-mail: inoue.kenichirou@nies.go.jp

Received May 28, 2008.
Accepted August 1, 2008.

DOI: 10.3181/0805-RM-179
1535-3702/08/23312-0001$15.00

components: washed DEP), and carbon nanoparticles enhance not only acute lung injury but systemic inflammation with coagulatory disturbance related to LPS (6, 11–13). Taken together, these findings demonstrate that environment-existing particles have aggravating effects on both lung and systemic inflammation with coagulopathy related to LPS.

The development of nano-technology has increased the risk of our exposure to types of particles other than combustion-derived particles in the environment, namely engineered nanomaterials (14). As these materials become more widespread, many questions arise as to the consequences that nanomaterials may have on the environment. In fact, previous reports showed that the full impact, or even partial impact, of manufactured nanomaterials on health and the environment has yet to be explored in depth (15–19). Among nanomaterials, carbon nanotubes (CNT) are unique. CNT possess significant characteristics in size (1–20 nm width, and many microns in length), strength, and surface chemistry (20). Notably, their length/width (aspect) ratios of > 1000, reactive surface chemistry, and/or poor solubility raise concerns linked to past experience with hazardous fibers, including asbestos. CNT exist in many forms, including single-walled CNT (SWCNT), double-walled, and multi-walled (MWCNT). Both SWCNT and MWCNT are being applied in wide-ranging areas from the semiconductor industry to drug delivery and super-light and strong composite materials (21) and are reportedly increasing in environmental exposure (22). The aim of the present study was therefore to experimentally elucidate whether two types of CNT (SWCNT and MWCNT) exacerbate lung and systemic inflammation with coagulatory disturbance induced by intratracheal administration of LPS in mice. In addition, effects of CNT on the production/release/expression of cytokines (tumor necrosis factor [TNF]-α and interleukin [IL]-1β) and chemokines (macrophage inflammatory protein [MIP]-1α, macrophage chemoattractant protein [MCP]-1, and keratinocyte-derived chemoattractant [KC]), which are reportedly induced by LPS and play an important role in local and systemic inflammation and/or coagulopathy both *in vivo* and *in vitro* (23, 24) to seek cellular mechanisms.

Materials and Methods

Animals. Male ICR mice, 6 weeks of age and weighing 28 to 33 g (Japan Clea Co., Tokyo, Japan) were used in all experiments. They were fed a commercial diet (Japan Clea Co.) and given water ad libitum. The mice were housed in an animal facility that was maintained at 24°C to 26°C with 55% to 75% humidity and a 12-h light/dark cycle.

CNT. Both SWCNT and MWCNT were purchased from SES Research (TX, USA). SWCNT were formed in a carbon arc in the presence of a metal catalyst. SWCNT ranged from 1.2–1.4 nm in diameter and 2–5 μm in length. MWCNT ranged from 2–20 nm in diameter, and 100 nm to several microns long with 5–20 graphitic layers. Both nanotubes were treated to open the ends of the nanotubes and to remove the amorphous carbon and nanoparticles. The end products contained up to 75% pure nanotubes and a larger percentage of open-ended tubes with the remaining material consisting of amorphous carbon and other carbon nanoparticles.

Study Protocol. Mice were divided into six experimental groups. The vehicle group received phosphate-buffered saline (PBS) at pH 7.4 (Invitrogen Co., Carlsbad, CA, USA) containing 1% Tween 80 (Nakalai Tesque, Tsukuba, Japan). The LPS group received 33 μg/kg of LPS (*E. coli.* B55:05, Difco Lab, Detroit, MI) dissolved in the vehicle. The CNT groups received 4 mg/kg of CNT (SWCNT or MWCNT) suspended in the same vehicle. The LPS + CNT groups received combined treatment using the same protocols as the LPS and CNT groups ($n = 20$–25 in each group). CNT were autoclaved at 250°C for 2 h before use, and the suspension was sonicated for 3 min using an Ultrasonic Disrupter (UD-201; Tomy Seiko, Tokyo, Japan). LPS activity, which was determined by Limulus Amebocyte Lysate assay (Seikagaku-kogyo, Tokyo, Japan), was lower than the detection limit (0.001 EU/ml) in the CNT after treatment. In each group, vehicle, CNT, LPS, or LPS + CNT were dissolved in 0.1-ml aliquots, and inoculated by the intratracheal route through a polyethylene tube under anesthesia with 4% halothane (Hoechst, Japan, Tokyo, Japan) as previously described (5, 6, 11–13, 25). The animals were studied 24 h after intratracheal administration. After deep anesthesia, the chest and abdominal walls were opened, and blood was retrieved by cardiac puncture. Blood samples were collected from the right ventricle with direct centrifugation for serum samples or into 3.8% sodium citrate in a ratio of 10:1 with centrifugation for plasma samples. After collection, bronchoalveolar lavage (BAL), pulmonary vascular permeability of water and protein, and protein levels of cytokines and chemokines in the lung tissue supernatants were examined. The studies adhered to the National Institutes of Health guidelines for the experimental use of animals. All animal studies were approved by the Institutional Review Board.

BAL, Pulmonary Vascular Permeability, Lung Histology, and Quantitation of Cytokine and Chemokine Protein Levels in Lung Tissue Supernatants. BAL and cell counts were conducted as previously described ($n = 8$ in each group) (5, 6, 11, 12). In a separate series of experiments, the lungs were weighed and dried as previously reported (3). The wet lung weight – the dry lung weight/body weight was calculated ($n = 8$ in each group). In another experiment, protein concentrations in BAL fluid were determined using the commercially available Bradford protein assay (Bio-Rad Laboratory Inc., Hercules, CA; $n = 8$ in each group) with bovine serum albumin as the standard. In another experiment, the lungs were fixed and stained with hematoxylin and eosin as previously described ($n = 4$–5 in

Table 1. The Number of Total Cells and Neutrophils, Protein Concentration in Bronchoalveolar Lavage (BAL) Fluid, and Lung Water Content After Intratracheal Challenge

Treatment	Total cells	Neutrophils	Protein	Lung wet weight - dry weight [mg]/body weight [g]
Vehicle	52.2 ± 3.6	1.6 ± 0.7	0.68 ± 0.04	4.44 ± 0.10
SWNT	88.4 ± 21.8*	35.8 ± 23.6**	1.55 ± 0.32**	6.46 ± 1.10**
MWCNT	68.8 ± 9.3	22.3 ± 5.9**	0.81 ± 0.05	4.43 ± 0.14
LPS	346.1 ± 35.6**	272.3 ± 26.9**	1.48 ± 0.07**	5.65 ± 0.18**
LPS + SWCNT	373.8 ± 40.4$^{**,\$}$	310.7 ± 31.2$^{**,\$}$	2.59 ± 0.30$^{**,\#,\$}$	7.41 ± 0.56$^{**,\#}$
LPS + MWCNT	356.4 ± 57.7$^{**,\$}$	299.2 ± 48.7$^{**,\$}$	1.73 ± 0.16$^{**,\$}$	6.03 ± 0.15$^{**,\$}$

* $P < 0.05$ vs. the vehicle group, ** $P < 0.01$ vs. the vehicle group, $^{\#}$ $P < 0.01$ vs. the LPS group, $^{\$}$ $P < 0.01$ vs the corresponding carbon nanotube (CNT) group.

each group) (5, 6, 13). ELISA for IL-1β, MIP-1α, MCP-1, and KC (R&D Systems, Minneapolis, MN, USA) in the lung tissue supernatants were conducted as previously described (6, 13), and the values were expressed as pg/total lung supernatants ($n = 8$ in each group).

Assays for Plasma Levels of Fibrinogen, von Willebrand Factor (vWF), Cytokines, Chemokines, and Activity of Protein C (APC). Plasma levels of fibrinogen and vWF, and the A PC ($n = 8$ in each group) were determined using commercial kits (Diagnostica Stargo, Roche, Tokyo, Japan) on STA Compact (Diagnostica Stargo, Roche) as described previously (26). Serum samples ($n = 8$ in each group) were analyzed by ELISA for TNF-α, IL-1β, MIP-1α, MCP-1, and KC (R&D Systems) according to the manufacturer's instructions, and the values were expressed as pg/ml.

Isolation, Culture, and Stimulation of Alveolar Macrophages (AM) and Peripheral Blood Monocytes (PBM). In another experiment, AM were isolated from ICR mice by BAL as previously described (27). All of the lavage fluid cells were pooled and spun at 1,200 *g* for 10 min. Lavage cells were pooled and counted after lysis of red blood cells with hypotonic solution. Heparinized blood was also obtained from ICR mice. All of the blood samples were pooled. Peripheral blood mononuclear cells were isolated by centrifugation on Ficoll-Paque (GE Healthcare Bio-Sciences AB, Uppsala, Sweden). Viability always exceeded 95% according to trypan blue exclusion. Cells were resuspended in RPMI 1640 medium (GIBCO BRL, Eggenstein, Germany) to give a concentration of 1×10^6 cells/ml. 20,000 cells were placed in each well of a 96-well culture plate (IWAKI microplate, ASAHI TECHNO GLASS, Funabashi, Japan) and washed with 200 μl of RPMI 1640 after 2 h, enabling the isolation of AM and PBM by adherence. CNT (1 μg/ml) with or without LPS (10 μg/ml) was then added to selected wells and incubated for 20 h. Culture supernatants were collected and the production of TNF-α, IL-1β, and KC was determined by ELISA as described above ($n = 3$ in each group). The experiment was repeated twice.

Statistical Analysis. Data are reported as the means ± SE. Differences between groups were determined using analysis of variance (ANOVA: Stat view version 4.0; Abacus Concepts, Inc., Berkeley, CA, USA) with Bonferroni comparison test. Differences were considered significant if $P < 0.05$.

Results

Effects of CNT on Airway Inflammation and Pulmonary Vascular Permeability. To investigate the magnitude of airway inflammation, we examined the cellular profile of BAL fluid 24 h after intratracheal instillation (Table 1). CNT alone increased the number of total cells and neutrophils as compared with vehicle ($P < 0.05$ for total cells with SWCNT, $P < 0.01$ for neutrophils). LPS exposure significantly increased the numbers as compared with vehicle exposure ($P < 0.01$). The numbers were greater in LPS + CNT groups than in the LPS group (NS) or the corresponding CNT groups ($P < 0.01$). To estimate pulmonary vascular permeability, we examined the protein levels in BAL fluid and the lung water content 24 h after intratracheal instillation (Table 1). Pulmonary exposure to SWCNT significantly elevated the protein levels of BAL fluid and the lung water content as compared to exposure to vehicle ($P < 0.01$). These values were significantly greater in the LPS group ($P < 0.01$) than in the vehicle group. These values were further greater in LPS + CNT groups than in the LPS group ($P < 0.01$ with SWCNT) or the corresponding CNT groups ($P < 0.01$, except for lung water content with LPS + SWCNT; NS).

Effects of CNT on Histological Changes in the Lung. To determine the effects of CNT on lung histology, we evaluated lung specimens stained with hematoxylin and eosin 24 h after intratracheal instillation (Fig. 1). No pathological change was seen in lungs obtained from the vehicle group. Infiltration of neutrophils was moderately seen in the lungs from CNT groups. Treatment with LPS or combined treatment with LPS and CNT showed marked infiltration of neutrophils into the lung parenchyma. Furthermore, the degree and extent were slightly greater in LPS + CNT groups than in the LPS group.

Effects of CNT on the Expression of Proinflammatory Cytokine and Chemokines in the

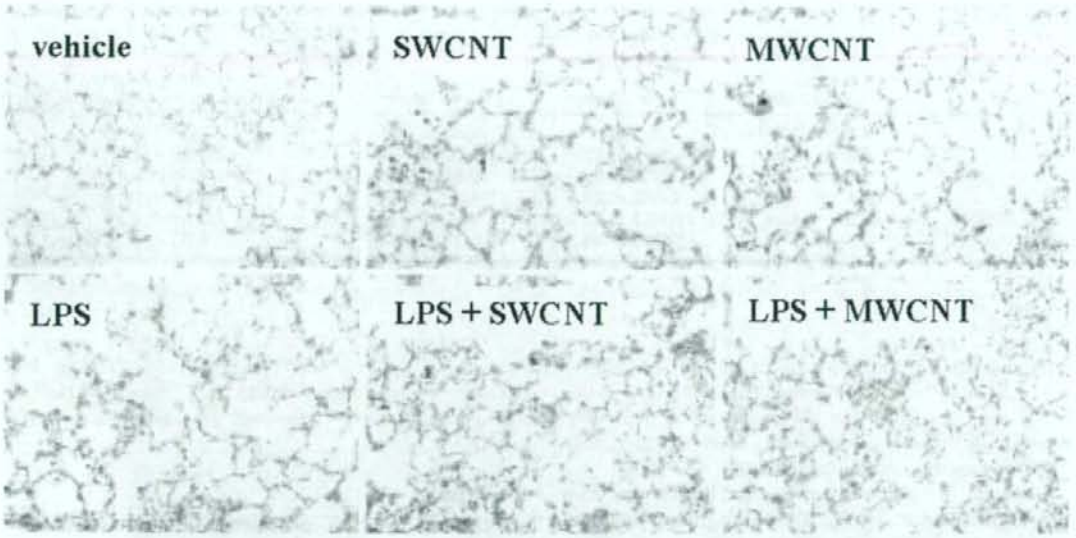

Figure 1. Histopathological findings of the lung. Twenty-four hours after intratracheal administration of vehicle, carbon nanotubes (carbon nanotubes: CNT [single-wall: SWCNT, and multi-wall: MWCNT]), lipopolysaccharide (LPS: 33 μg/kg), or LPS + CNT, mice were killed and lung histology was assessed by hematoxylin and eosin stain ($n = 4$–5 in each group). Original magnification, ×400.

Lung. To investigate the effects of CNT on local cytokine and chemokine expression, we next measured the protein levels of IL-1β, MIP-1α, MCP-1, and KC in lung tissue supernatants 24 h after intratracheal instillation (Table 2). Pulmonary exposure to CNT alone significantly elevated the levels of IL-1β, MIP-1α, and MCP-1 as compared to exposure to vehicle ($P < 0.01$). On the other hand, LPS challenge significantly elevated the levels of all of the proteins as compared with vehicle challenge ($P < 0.01$). These levels were significantly greater in LPS + CNT groups than in the corresponding CNT groups ($P < 0.01$). The IL-1β level was comparable among the LPS and LPS + CNT groups. The other levels were greater in the LPS + CNT groups than in the LPS; however, the difference did not reach statistical significance except for KC with the LPS + MWCNT ($P < 0.05$).

Effects of CNT on Coagulatory Changes. To elucidate the impact of pulmonary exposure to CNT on the coagulatory system, we next analyzed coagulatory parameters 24 h after intratracheal challenge (Table 3). SWCNT exposure significantly elevated the fibrinogen level as compared to vehicle exposure ($P < 0.01$). LPS challenge significantly elevated the values as compared to vehicle challenge ($P < 0.05$). The values were further greater in LPS + CNT groups than in the LPS group ($P < 0.01$ with LPS + SWCNT) or the corresponding CNT groups ($P < 0.01$). As compared to vehicle challenge, LPS, SWCNT, and LPS + SWCNT challenge caused an increase in the level of vWF without statistical significance. CNT, LPS, and LPS + MWCNT decreased APC as compared with vehicle ($P < 0.01$ with SWCNT and LPS + CNT). Activity was further decreased in the LPS + SWCNT group than in the LPS group ($P < 0.01$) or the corresponding CNT group (NS).

Effects of CNT on Circulatory Levels of Proinflammatory Cytokine and Chemokines. To investi-

Table 2. Protein Levels of Interleukin (IL)-1β and Chemokines in the Lung Tissue Supernatants After Intratracheal Challenge

Treatment	IL-1β	MIP-1α	MCP-1	KC
Vehicle	182.6 ± 22.2	2.1 ± 1.2	12.0 ± 2.1	129.5 ± 78.7
SWCNT	1248.6 ± 556.2*	67.7 ± 27.2*	128.1 ± 46.0*	207.9 ± 112.4
MWCNT	673.8 ± 184.3*	53.1 ± 12.6*	53.5 ± 7.3*	244.1 ± 76.6
LPS	6320.0 ± 342.7*	788.8 ± 101.6*	659.8 ± 129.5*	1246.8 ± 147.2*
LPS + SWCNT	6132.3 ± 547.2*,$	946.5 ± 109.5*,$	791.8 ± 180.1*,$	1370.8 ± 193.4*,$
LPS + MWCNT	5390.9 ± 339.6*,$	948.8 ± 146.4*,$	948.9 ± 166.2*,$	1735.6 ± 276.0*,#,$

* $P < 0.01$ vs. the vehicle group, # $P < 0.05$ vs. the LPS group, $ $P < 0.01$ vs. the corresponding CNT group.

Table 3. Plasma Coagulatory Parameters After Intratracheal Instillation

Treatment	Fibrinogen	vWF	APC
Vehicle	318.3 ± 8.4	99.0 ± 5.2	5.6 ± 0.2
SWCNT	451.8 ± 50.1**	112.3 ± 6.4	4.1 ± 0.4**
MWCNT	340.4 ± 13.0	91.6 ± 4.0	5.0 ± 0.3
LPS	439.0 ± 27.3*	100.0 ± 3.5	4.6 ± 0.3**
LPS + SWCNT	626.3 ± 50.8**,##,§	106.5 ± 4.8	3.6 ± 0.2**,##
LPS + MWCNT	526.5 ± 30.4**,§	97.4 ± 7.2	4.6 ± 0.3**

* $P < 0.05$ vs. the vehicle group, ** $P < 0.01$ vs. the vehicle group, # $P < 0.05$ vs. the LPS group, ## $P < 0.01$ vs. the LPS group, § $P < 0.01$ vs. the corresponding CNT group.

gate the circulatory levels of cytokine and chemokines, we measured the protein levels of TNF-α, IL-1β, MIP-1α, MCP-1, and KC in the sera 24 h after intratracheal instillation (Table 4). CNT or LPS challenge did not alter these levels as compared to vehicle challenge; however, these levels were greater in the LPS + CNT groups, particularly, the LPS + SWCNT group than in the vehicle group ($P < 0.01$ for IL-1β and MCP-1; $P < 0.05$ for MIP-1α and KC). The levels were further greater in LPS + SWCNT groups than in the LPS ($P < 0.01$ for IL-1β; $P < 0.05$ for MIP-1α and KC), or the CNT ($P < 0.01$ for MCP-1; $P < 0.05$ for KC) group.

Effects of CNT on Functions of AM and PBM. To assess the effects of CNT on functions of AM and PBM in terms of cytokine production, we harvested AM and PBM from naïve ICR mice, and then stimulated with LPS (10 μg/ml) or medium alone *in vitro* for 20 h in the presence or absence of CNT, and determined protein levels for IL-1β, TNF-α, and KC (Fig. 2). SWCNT exposure moderately elevated the IL-1β level in AM culture, although it did not reach statistical significance. LPS elevated all the levels by AM ($P < 0.01$ for TNF-α and KC). The levels for all cytokines by LPS + CNT- exposed AM were comparable to those by LPS-exposed AM. CNT exposure did not elevate the IL-1β level by PBM as compared to medium exposure. LPS moderately elevated all of the levels without significance. The levels were greater by LPS + CNT-exposed PBM than by LPS-exposed PBM ($P < 0.01$ for TNF-α, $P < 0.05$ for IL-1β).

Discussion

The present study has demonstrated that 1) pulmonary exposure to two types of CNT, particularly SWCNT, induces neutrophilic lung inflammation and pulmonary edema with enhanced lung expression of proinflammatory cytokines; 2) however, they do not significantly enhance LPS-elicited lung inflammation; 3) SWCNT induce systemic inflammation, and augment systemic inflammation with coagulopathy accompanied by lung inflammation induced by LPS; and 4) finally, CNT amplified LPS-induced cytokine production from PBM.

Short-term exposure to ambient PM is related to mortality and morbidity in individuals with cardiopulmonary predisposing factors (28–30). Consistent with epidemiological studies, we previously demonstrated that DEP, important constituents of $PM_{2.5}$, and carbon nanoparticles enhance lung inflammation related to LPS (6, 11, 13) and the accompanying systemic inflammation with coagulatory disturbance (12, 13) using the same protocol as that in the present study. Furthermore, we demonstrated that carbon nanoparticles, used as a type of ambient PM, deteriorate lung inflammation and subsequent systemic inflammation with coagulatory disturbance in the same model as used in the present study (13). Collectively, environment-existing particles play roles in the adverse effects on cardiopulmonary systems with predisposing factors such as lung and systemic inflammation and the resultant coagulopathy. On the other hand, industry-engineered materials have reportedly been increasing in the environment as well as combustion-derived nanoparticles (16, 17); thus, it can be imagined that exposure to these materials, especially nano-

Table 4. Circulatory Levels of Cytokines and Chemokines After Intratracheal Instillation

Treatment	TNF-α	IL-1β	MIP-1α	MCP-1	KC
Vehicle	4.4 ± 0.4	8.5 ± 0.4	20.4 ± 0.5	131.2 ± 3.0	164.7 ± 5.3
SWCNT	4.7 ± 0.7	15.7 ± 1.3	28.2 ± 4.7	134.0 ± 2.9	174.9 ± 6.3
MWCNT	4.6 ± 0.5	12.0 ± 1.4	20.8 ± 0.8	159.5 ± 8.9**	213.0 ± 28.0*
LPS	4.3 ± 0.6	10.0 ± 0.6	20.3 ± 0.6	149.0 ± 4.2*	170.1 ± 9.7
LPS + SWCNT	10.2 ± 3.7	24.0 ± 7.7**,##	29.6 ± 4.1*,#	156.6 ± 5.5**,§§	242.9 ± 39.3*,#,§
LPS + MWCNT	8.4 ± 2.3	10.5 ± 0.6	21.9 ± 0.8	148.5 ± 4.3*	218.7 ± 7.6

* $P < 0.05$ vs. the vehicle group, ** $P < 0.01$ vs. the vehicle group, # $P < 0.05$ vs. the LPS group, ## $P < 0.01$ vs. the LPS group, § $P < 0.01$ vs. the corresponding CNT group.

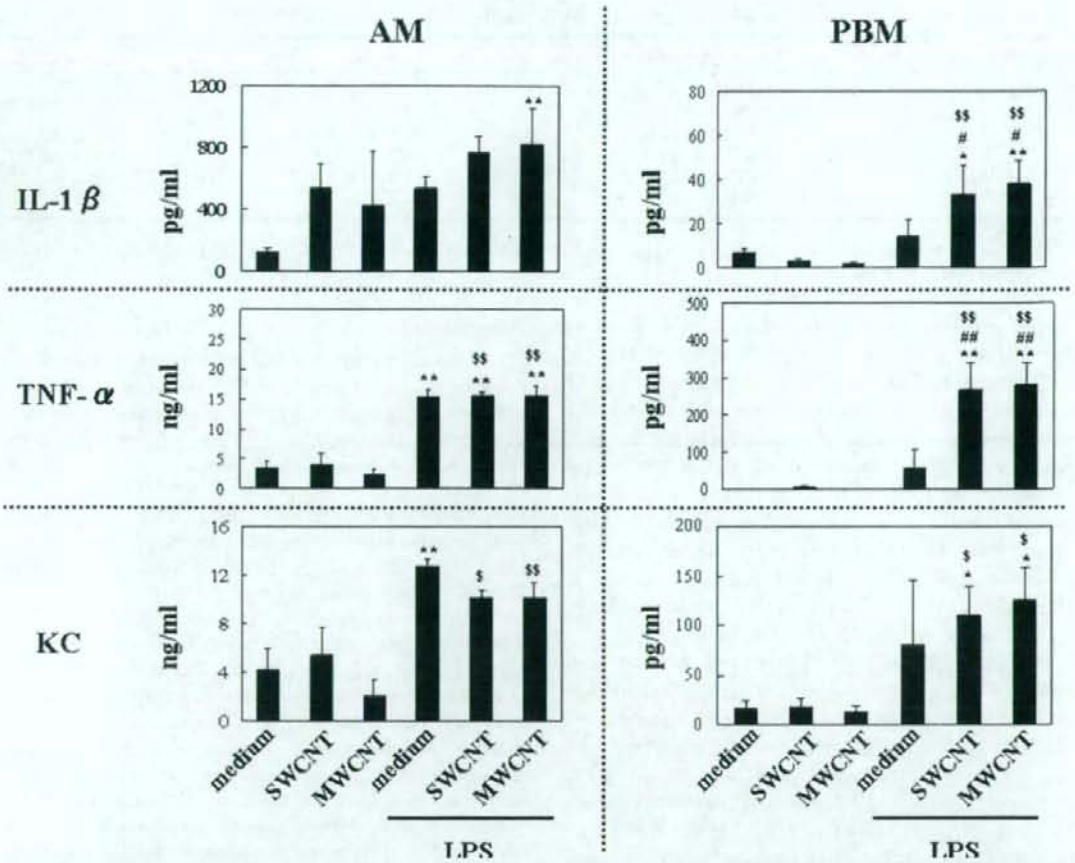

Figure 2. Cytokine production by alveolar macrophage (AM) and peripheral blood monocytes (PBM) in response to lipopolysaccharide (LPS) and/or carbon nanotubes (CNT). AM and PBM were isolated from naïve ICR mice, purified with adherence, and then stimulated *in vitro* with LPS (10 μg/ml) or with medium alone in the presence or absence of CNT for 20 h. Culture supernatants were collected for the determination of interleukin (IL)-1β, tumor necrosis factor (TNF)-α, and keratinocyte-derived chemoattractant (KC) levels by ELISA. * $P < 0.05$ vs. medium, ** $P < 0.01$ vs. medium, $^{\#}$ $P < 0.05$ vs. LPS, $^{\#\#}$ $P < 0.01$ vs. LPS, $^{\$}$ $P < 0.05$ vs. CNT, $^{\$\$}$ $P < 0.01$ vs. CNT. Results are representative of two independent experiments; $n = 3$ per condition.

sized materials, also has adverse health effects, especially inflammatory conditions. Indeed, Warheit and colleagues have demonstrated that a single intratracheal administration of 300 nm TiO_2 induces lung inflammation (31). Furthermore, a recent study has shown that a single pulmonary exposure to nano TiO_2 particles (19–21 nm) induces emphysema-like lung injury (32). Also, SWCNT instilled through the airways (pharynges) induce lung inflammation, which is characterized by fibrogenic changes with granuloma formation (33). Consistent with these previous reports, our study also showed that CNT alone induced the apparent acute type of neutrophilic lung inflammation (Table 1). On the other hand, all previous studies examined the effects of (nano) materials on normal subjects/conditions in terms of toxicity, including carcinogenesis. Further, importantly, there was no report about the effects of pulmonary-exposed nanomaterials on coagulatory systems. The present results, for the first time to our knowledge, showed that exposure to two types (SWCNT and MWCNT) of manufactured CNT can facilitate both local (*i.e.*, lung) inflammation with edema and systemic inflammation with coagulatory disturbance induced by LPS.

Nano-sized particles/materials are reportedly able to affect not only the respiratory tract but also the systemic circulation (14, 34, 35), implying that they can affect the circulatory system. In accord with these studies, we previously demonstrated that carbon nanoparticles enhance systemic inflammation with coagulatory disturbance in the same model as used in the present study (13). In addition, enhancement has been greater with smaller than larger

nanoparticles (13). In this respect, a recent study by another group has shown that pulmonary exposure to MWCNT elevates circulatory levels of procoagulant microvesicular tissue factor (TF) activity, implying their enhanced thrombogenicity (36). Further, Li *et al.* have recently demonstrated that airway exposure to SWCNT induces mitochondrial damage in the aorta of wild-type mice and accelerates atherosclerosis formation in ApoE$^{-/-}$ mice (37). In the present study, LPS combined with CNT, specifically with SWCNT, significantly elevated the levels of fibrinogen, IL-1β, MCP-1, and KC in circulating blood compared to LPS alone. Additionally, the decrease in APC induced by LPS was further repressed by the combination of LPS with SWCNT. These findings suggest that CNT, especially SWCNT, can directly and/or indirectly promote systemic inflammation with coagulatory disturbance accompanied by lung inflammation, similar to nanoparticles (13). Interestingly, the degree of promotion was apparently greater in systemic inflammation with coagulopathy than in lung inflammation (Tables 1, 3, 4). It can be hypothesized that endothelial-epithelial damage induced by CNT and subsequent infiltrated effector leukocytes allow large amounts of LPS (and CNT) to pass easily into the circulation, resulting in synergistic effects on systemic inflammation and hemostasis, including coagulatory disturbance. The marked enhancing effects of SWCNT on LPS-elicited pulmonary vascular permeability might, at least in part, support this concept. Otherwise, we have previously shown by electron microscopy that intratracheally instilled carbon nanoparticles occasionally pass into the circulation through the large gap formed between alveolar epithelial cells (38). It is possible that the gap is formed as a result of shrinkage of the cytoplasm, by receiving stimulus/signals generated following nanoparticle attachment on these cells (38). Thus, it can also be proposed that SWCNT's attachment to alveolar epithelial cells enlarges the gap. Alternately, their unique shapes (fibrous with a nano-leveled cross section) may make it easier to pass through the endothelial-epithelial barrier with or without LPS and consequently to induce/augment systemic inflammation with coagulatory disturbance. In this regard, persistent reactive fibers reportedly lead to oxidative reactions (39), important reactions in vascular pathophysiology including coagulatory disorders (40). In any case, these observations may shed light on their facilitating properties of systemic inflammation with coagulopathy as well as the dynamics of (SW) CNT from the airways to the circulation, and further studies are needed to address these important issues and their mechanisms.

Innate immunity including the response against LPS initiates from macrophage/monocyte activation. Furthermore, LPS induces macrophages/monocytes to express TF, which results in intravascular fibrin deposition through activation of the coagulation protease cascade (41). To rationally explain the effects of CNT on LPS-related lung and systemic pathology, we isolated AM and PBM from the animals and cultured with LPS and/or CNT. As a result, CNT did not synergistically amplify LPS-evoked cytokine production by AM but did by PBM. Thus, the *in vitro* findings were partly linked to the *in vivo* observation that CNT did not significantly exacerbate LPS-elicited lung inflammation but rather accompanied systemic inflammation and coagulatory disturbance. Taken together, the *in vivo* effects of CNT may be in part explained by their impact on macrophage/monocyte populations. In other words, this simple *in vitro* assay system using AM and PBM might be suitable for screening the facilitating effects of toxic pollutants on this *in vivo* model and/or human inflammatory diseases (i.e. SIRS) with coagulopathy. On the other hand, however, there existed discrepant findings between *in vivo* and *in vitro* studies, especially with those on MWCNT. In fact, MWCNT did not significantly enhance systemic inflammation and coagulatory disturbance, but did LPS-induced cytokine production *in vitro*. The reason of the phenomenon remains unclarified. This may be explained by disability of the CNT to translocate from the lung into circulation, resulting in minor facilitation against systemic inflammatory responses *in vivo*. Additional studies are needed to address the issue.

In conclusion, this study demonstrated that pulmonary exposure to CNT moderately exacerbated/amplified lung inflammation, pulmonary vascular permeability, and lung expression of proinflammatory cytokines induced by LPS. The enhancing effects were more apparent with the single-walled type (SWCNT) than with multi-walled type (MWCNT) in overall trend. Furthermore, SWCNT also enhanced systemic inflammation and, more importantly, coagulatory disturbance accompanying lung inflammation. These results suggest that CNT can facilitate lung inflammation related to LPS and consequent systemic inflammation with coagulopathy. These aggravating effects of CNT might play a vital role in the adverse health effects of industrial nanomaterials on sensitive individuals with cardiovascular and respiratory diseases, including atherosclerosis and respiratory infection.

1. Gando S, Tedo I. Increased neutrophil elastase release in patients with cardiopulmonary arrest: role of elastase inhibitor. Intensive Care Med 21:636–640, 1995.
2. Dockery DW, Pope CA 3rd. Acute respiratory effects of particulate air pollution. Annu Rev Public Health 15:107–132, 1994.
3. Ichinose T, Furuyama A, Sagai M. Biological effects of diesel exhaust particles (DEP). II. Acute toxicity of DEP introduced into lung by intratracheal instillation. Toxicology 99:153–167, 1995.
4. Ichinose T, Yajima Y, Nagashima M, Takenoshita S, Nagamachi Y, Sagai M. Lung carcinogenesis and formation of 8-hydroxy-deoxyguanosine in mice by diesel exhaust particles. Carcinogenesis 18:185–192, 1997.
5. Takano H, Yoshikawa T, Ichinose T, Miyabara Y, Imaoka K, Sagai M. Diesel exhaust particles enhance antigen-induced airway inflammation and local cytokine expression in mice. Am J Respir Crit Care Med 156: 36–42, 1997.
6. Takano H, Yanagisawa R, Ichinose T, Sadakane K, Yoshino S, Yoshikawa T, Morita M. Diesel exhaust particles enhance lung injury

related to bacterial endotoxin through expression of proinflammatory cytokines, chemokines, and intercellular adhesion molecule-1. Am J Respir Crit Care Med 165:1329–1335, 2002.

7. Forastiere F, Stafoggia M, Picciotto S, Bellander T, D'Ippoliti D, Lanki T, von Klot S, Nyberg F, Paatero P, Peters A, Pekkanen J, Sunyer J, Perucci CA. A case-crossover analysis of out-of-hospital coronary deaths and air pollution in Rome, Italy. Am J Respir Crit Care Med 172:1549–1555, 2005.
8. Yue W, Schneider A, Stolzel M, Ruckerl R, Cyrys J, Pan X, Zereba W, Koenig W, Wichmann HE, Peters A. Ambient source-specific particles are associated with prolonged repolarization and increased levels of inflammation in male coronary artery disease patients. Mutat Res 621: 50–60, 2007.
9. Dockery DW, Pope CA 3rd, Xu X, Spengler JD, Ware JH, Fay ME, Ferris BG Jr, Speizer FE. An association between air pollution and mortality in six U.S. cities. N Engl J Med 329:1753–1759, 1993.
10. Becker S, Fenton MJ, Soukup JM. Involvement of microbial components and toll-like receptors 2 and 4 in cytokine responses to air pollution particles. Am J Respir Cell Mol Biol 27:611–618, 2002.
11. Yanagisawa R, Takano H, Inoue K, Ichinose T, Sadakane K, Yoshino S, Yamaki K, Kumagai Y, Uchiyama K, Yoshikawa T, Morita M. Enhancement of acute lung injury related to bacterial endotoxin by components of diesel exhaust particles. Thorax 58:605–612, 2003.
12. Inoue K, Takano H, Sakurai M, Oda T, Tamura H, Yanagisawa R, Shimada A, Yoshikawa T. Pulmonary exposure to diesel exhaust particles enhances coagulatory disturbance with endothelial damage and systemic inflammation related to lung inflammation. Exp Biol Med (Maywood) 231:1626–1632, 2006.
13. Inoue K, Takano H, Yanagisawa R, Hirano S, Sakurai M, Shimada A, Yoshikawa T. Effects of airway exposure to nanoparticles on lung inflammation induced by bacterial endotoxin in mice. Environ Health Perspect 114:1325–1330, 2006.
14. Oberdorster G, Oberdorster E, Oberdorster J. Nanotoxicology: an emerging discipline evolving from studies of ultrafine particles. Environ Health Perspect 113:823–839, 2005.
15. Borm PJ. Particle toxicology: from coal mining to nanotechnology. Inhal Toxicol 14:311–324, 2002.
16. Colvin VL. The potential environmental impact of engineered nanomaterials. Nat Biotechnol 21:1166–1170, 2003.
17. Guzman KA, Taylor MR, Banfield JF. Environmental risks of nanotechnology: National Nanotechnology Initiative funding, 2000–2004. Environ Sci Technol 40:1401–1407, 2006.
18. Hardman R. A toxicologic review of quantum dots: toxicity depends on physicochemical and environmental factors. Environ Health Perspect 114:165–172, 2006.
19. Nel A, Xia T, Madler L, Li N. Toxic potential of materials at the nanolevel. Science 311:622–627, 2006.
20. Mitchell LA, Gao J, Wal RV, Gigliotti A, Burchiel SW, McDonald JD. Pulmonary and systemic immune response to inhaled multiwalled carbon nanotubes. Toxicol Sci 100:203–214, 2007.
21. de Jonge N, Bonard JM. Carbon nanotube electron sources and applications. Philos Transact A Math Phys Eng Sci 362:2239–2266, 2004.
22. Muller J, Huaux F, Moreau N, Misson P, Heilier JF, Delos M, Arras M, Fonseca A, Nagy JB, Lison D. Respiratory toxicity of multi-wall carbon nanotubes. Toxicol Appl Pharmacol 207:221–231, 2005.
23. Kopydlowski KM, Salkowski CA, Cody MJ, van Rooijen N, Major J, Hamilton TA, Vogel SN. Regulation of macrophage chemokine expression by lipopolysaccharide in vitro and in vivo. J Immunol 163:1537–1544, 1999.
24. Salgado A, Boveda JL, Monasterio J, Segura RM, Mourelle M, Gomez-Jimenez J, Peracaula R. Inflammatory mediators and their influence on haemostasis. Haemostasis 24:132–138, 1994.
25. Inoue KI, Takano H, Yanagisawa R, Hirano S, Kobayashi T, Ichinose T, Yoshikawa T. Effects of organic chemicals derived from ambient particulate matter on lung inflammation related to lipopolysaccharide. Arch Toxicol 80:833–838, 2006.
26. Inoue K, Takano H, Yanagisawa R, Sakurai M, Shimada A, Morita T, Sato M, Yoshino S, Yoshikawa T, Tohyama C. Protective role of interleukin-6 in coagulatory and hemostatic disturbance induced by lipopolysaccharide in mice. Thromb Haemost 91:1194–1201, 2004.
27. Bissonnette E, Carre B, Dubois C, Rola-Pleszczynski M. Inhibition of alveolar macrophage cytotoxicity by asbestos: possible role of prostaglandins. J Leukoc Biol 47:129–134, 1990.
28. Brook RD, Franklin B, Cascio W, Hong Y, Howard G, Lipsett M, Luepker R, Mittleman M, Samet J, Smith SC Jr, Tager I: Expert Panel on Population and Prevention Science of the American Heart Association. Air pollution and cardiovascular disease: a statement for healthcare professionals from the Expert Panel on Population and Prevention Science of the American Heart Association. Circulation 109:2655–2671, 2004.
29. Peters A, Wichmann HE, Tuch T, Heinrich J, Heyder J. Respiratory effects are associated with the number of ultrafine particles. Am J Respir Crit Care Med 155:1376–1383, 1997.
30. Samet JM, Dominici F, Curriero FC, Coursac I, Zeger SL. Fine particulate air pollution and mortality in 20 U.S. cities, 1987–1994. N Engl J Med 343:1742–1749, 2000.
31. Warheit DB, Webb TR, Sayes CM, Colvin VL, Reed KL. Pulmonary instillation studies with nanoscale TiO2 rods and dots in rats: toxicity is not dependent upon particle size and surface area. Toxicol Sci 91:227–236, 2006.
32. Chen HW, Su SF, Chien CT, Lin WH, Yu SL, Chou CC, Chen JJ, Yang PC. Titanium dioxide nanoparticles induce emphysema-like lung injury in mice. FASEB J 20:2393–2395, 2006.
33. Shvedova AA, Kisin ER, Mercer R, Murray AR, Johnson VJ, Potapovich AI, Tyurina YY, Gorelik O, Arepalli S, Schwegler-Berry D, Hubbs AF, Antonini J, Evans DE, Ku BK, Ramsey D, Maynard A, Kagan VE, Castranova V, Baron P. Unusual inflammatory and fibrogenic pulmonary responses to single-walled carbon nanotubes in mice. Am J Physiol Lung Cell Mol Physiol 289:L698–L708, 2005.
34. MacNee W, Donaldson K. How can ultrafine particles be responsible for increased mortality? Monaldi Arch Chest Dis 55:135–139, 2000.
35. Nemmar A, Vanbilloen H, Hoylaerts MF, Hoet PH, Verbruggen A, Nemery B. Passage of intratracheally instilled ultrafine particles from the lung into the systemic circulation in hamster. Am J Respir Crit Care Med 164:1665–1668, 2001.
36. Nemmar A, Hoet PH, Vandervoort P, Dinsdale D, Nemery B, Hoylaerts MF. Enhanced peripheral thrombogenicity after lung inflammation is mediated by platelet-leukocyte activation: role of P-selectin. J Thromb Haemost 5:1217–1226, 2007.
37. Li Z, Hulderman T, Salmen R, Chapman R, Leonard SS, Young SH, Shvedova A, Luster MI, Simeonova PP. Cardiovascular effects of pulmonary exposure to single-wall carbon nanotubes. Environ Health Perspect 115:377–382, 2007.
38. Shimada A, Kawamura N, Okajima M, Kaewamatawong T, Inoue H, Morita T. Translocation pathway of the intratracheally instilled ultrafine particles from the lung into the blood circulation in the mouse. Toxicol Pathol 34:949–957, 2006.
39. McClellan RO. Assessing health risks of synthetic vitreous fibers: an integrative approach. Regul Toxicol Pharmacol 20:S121–S134, 1994.
40. Walford G, Loscalzo J. Nitric oxide in vascular biology. J Thromb Haemost 1:2112–2118, 2003.
41. Pawlinski R, Pedersen B, Schabbauer G, Tencati M, Holscher T, Boisvert W, *et al.* Role of tissue factor and protease-activated receptors in a mouse model of endotoxemia. Blood 103:1342–1347, 2004.

SIZE EFFECTS OF NANOMATERIALS ON LUNG INFLAMMATION AND COAGULATORY DISTURBANCE

K. INOUE[1], H. TAKANO[1,2], M. OHNUKI[1], R. YANAGISAWA[1], M. SAKURAI[1], A. SHIMADA[3], K. MIZUSHIMA[2] and T. YOSHIKAWA[2]

[1]Environmental Health Sciences Division, National Institute for Environmental Studies, Ibaraki; [2]Inflammation and Immunology, Graduate School of Medical Science, Kyoto Prefectural University of Medicine, Kyoto; [3]Department of Veterinary Pathology, Faculty of Agriculture, Tottori University, Tottori, Japan

Effects of nano-sized materials (nanomaterials) on subjects with predisposing inflammatory disorders have not been well elucidated. This study examines the effects of pulmonary exposure to TiO_2 nanomaterials on lung inflammation induced by lipopolysaccharide (LPS) and consequent systemic inflammation with coagulatory disturbance in mice, in particular regarding their size-dependency. Also, gene expression pattern in the lung was compared among the experimental groups using cDNA microarray analysis. ICR male mice were divided into 8 experimental groups that intratracheally received vehicle, three sizes (15, 50, 100 nm) of TiO_2 nanomaterials (8 mg/kg), LPS (2.5 mg/kg), or LPS plus nanomaterials. Twenty four h after the treatment, both nanomaterials exacerbated the lung inflammation and vascular permeability elicited by LPS, with an overall trend of amplified lung expressions of cytokines such as interleukin (IL)-1β, macrophage chemoattractant protein (MCP)-1, and keratinocyte chemoattractant (KC). LPS plus nanomaterials, especially of a size less than 50 nm, elevated circulatory levels of fibrinogen, IL-1 β, MCP-1, and KC, and von Willebrand factor as compared with LPS alone. The enhancement tended overall to be greater with the smaller nanomaterials than with the larger ones. cDNA microarray analyses revealed that there was no difference in gene expression pattern between the LPS group and the LPS + nanomaterial groups. These results suggest that nanomaterials exacerbate lung inflammation related to LPS with systemic inflammation and coagulatory disturbance, and that the exacerbation is more prominent with smaller nanomaterials than with larger ones.

Environmental particulate matters (PM) are well recognized to be toxic for health, including the respiratory systems (1). In particular, diesel exhaust particles (DEP), main contributors to environmental PM in urban areas, reportedly not only induce lung inflammation and/or cancer (2-3) but facilitate several respiratory diseases such as bronchial asthma and acute lung injury (2-5). Our previous studies have demonstrated that DEP and their components (especially residual particles after extraction of chemical components; referred to as "washed DEP") enhance acute lung inflammation related to lipopolysaccharide (LPS) (5-6). Furthermore, washed DEP were shown to augment systemic inflammation and coagulatory disturbance accompanied by lung inflammation (7). More recently, we demonstrated that carbon nanoparticles (less than 100 nm in size) exacerbate lung inflammation with systemic

Key words: TiO_2 nanomaterials, lung inflammation, LPS, coagulatory disturbance, systemic inflammation

Mailing address: Ken-ichiro Inoue, MD, PhD, Environmental Health Sciences Division, National Institute for Environmental Studies, 16-2 Onogawa, Tsukuba, 305-8506, Japan
Tel /Fax: ++81 298 50 2334
e-mail: inoue.kenichirou@nies.go.jp

0394-6320 (2008)

inflammation and coagulatory disturbance in mice (8). Taken together, these findings demonstrated that pulmonary exposure to environment-existing particles causes aggravating effects on lung inflammation and consequent systemic inflammation with coagulatory disturbance.

The development of nano-technology has increased the risk of types of particles other than those combustion-derived in the environment, namely, engineered nanomaterials (9). Considering the variety of their size and nature, it can be supposed that exposure to nano-level (< 100 nmm) materials might also lead to adverse health effects, including cardiorespiratory ones. Indeed, health toxicity induced by nanomaterials is being researched worldwide. In particular, nanomaterial exposure reportedly induces several patterns of lung inflammation (10-14). However, the effects of nanomaterials on subjects with predisposing inflammatory disorders have not been elucidated as far as we know. Furthermore, comparative studies of the size effects of pulmonary exposure to nanomaterials on subjects with predisposing factors, such as lung inflammation related to LPS, have never been carried out.

Titanium has been used clinically as an implant material (15). Furthermore, TiO_2 nanomaterials are widely used as photocatalysts in air and water cleansing (16). These facts suggest that the ambient and/or local concentrations of these materials may increase in the future. The present study is, therefore, designed to elucidate the effects of three sizes of TiO_2 nanomaterials on lung inflammation induced by intratracheal administration of LPS. We also investigated the local expression of cytokines and chemokines in the lung and serum. Furthermore, we examined the effects of pulmonary exposure to nanomaterials on coagulatory changes in the presence or absence of LPS. Finally, we examined the gene expression pattern in the lung to explore the underlying mechanisms of the adverse effects.

MATERIALS AND METHODS

Animals

184 male ICR mice 6 wks of age and weighing 29 to 33 g (Japan Clea Co., Tokyo, Japan) were used in all experiments. They were fed a commercial diet (Japan Clea Co.) and given water ad libitum. The mice were housed in an animal facility that was maintained at 24-26□ with 55-75% humidity and a 12-h light/dark cycle.

Study protocol

The mice were divided into eight experimental groups (20-25 per group). The vehicle group received sterile saline (Nissui Pharmaceutical Co). The LPS group received 2.5 mg/kg of LPS (*E. coli.* B55:05, Difco Lab, Detroit, MI) dissolved in the vehicle. The TiO_2 nanomaterial groups received 8 mg/kg of TiO_2 (15 nm, 50 nm, or 100 nm: Nakalai Tesque, Kyoto, Japan) suspended in the same vehicle. The LPS + TiO_2 groups received combined treatment using the same protocols as the LPS and the nanomaterial groups (n = 20-25 in each group). The size of each particle was measured using a JEM-2010 transmission electron microscope (TEM; JEOL, Tokyo, Japan). TiO_2 nanomaterials were autoclaved at 250□ for 2 h before use, and the suspension was sonicated for 3 min using an Ultrasonic disrupter (UD-201; Tomy Seiko, Tokyo, Japan). Vehicle, nanomaterials, LPS, or LPS + nanomaterials were dissolved in 0.1-ml aliquots, and inoculated by the intratracheal route through a polyethylene tube under anesthesia with 4% halothane (Hoechst, Japan, Tokyo, Japan). The animals were studied 24 h after the intratracheal administration with bronchoalveolar lavage (BAL), pulmonary vascular permeability of water and protein, lung histology, protein levels of cytokines and chemokines in the lung tissue supernatants and the sera, and parameters related to coagulatory system. The animals were also examined by DNA microarray analysis 4 h after the intratracheal administration. The studies adhered to the National Institutes of Health guidelines for the experimental use of animals. All animal studies were approved by the Institutional Review Board.

BAL, pulmonary vascular permeability, lung histology, and quantitation of cytokine and chemokine protein levels in the lung tissue supernatants

BAL and cell counts were conducted as previously described (n = 8 in each group) (4-6, 8). In a separate series of experiments, the lungs were weighed and dried as previously reported (2). The wet lung weight – the dry lung weight/body weight was calculated (n = 8 in each group). In another experiment, protein concentrations in BAL fluid were determined using the commercially available Bradford protein assay (Bio-Rad Laboratory Inc., Hercules, CA: n = 8 in each group) with bovine serum albumin as the standard. In another experiment, the lungs were fixed and stained with hematoxylin and eosin as previously described (4-5, 8). Polymorphonuclear leukocyte (PMN) infiltration was assessed by averaging the number of neutrophils enumerated in 30 randomly selected high power fields (HPFs; ×400) in each slide. Histologic sections were evaluated in a blind